Proceeding of the IEEE
International Conference on Robotics and Biomimetics
Dali, China, December 2019

An Aerodynamics Calculation Method of a Flapping Wing Flying Robot Based on State-Space Airloads Theory*

Hui Xu, Erzhen Pan, Dong Xue, Wenfu Xu*, Senior, *IEEE*, Yuanpeng Wang, Xu Liang

School of Mechanical Engineering and Automation
Harbin Institute of Technology, Shenzhen
Shenzhen, Guangdong Province, China
xuhui@stu.hit.edu.cn; panerzhen@stu.hit.edu.cn; xuedong@hit.edu.cn
wfxu@hit.edu.cn; 18S053167@stu.hit.edu.cn; 249669522@qq.com

***Abstract* – The creation of Flapping-wing aerial vehicles (FAVs) which mimic birds to fly by flapping its wings spawns renewed interest in flapping wing flight. How aerodynamic loads are produced by flapping wings is one of the key issues to design high-performance FAVs. This paper develops a method for calculating flapping aerodynamic loads based on state-space airloads theory and calculates the aerodynamic loads of our FAV HITHawk in different working conditions. Besides, a series of experiments are designed to validate the accuracy of this method. The comparison results showed that this method provides a good accuracy for lift calculation, while the thrust calculation results do not match the experimental results commendably.**

Index Terms* – *FAV, thin airfoil theory, HITHawk, robotic bird.

I. INTRODUCTION

Birds, bats and insects fly by flapping their wings have fascinated humans for many years. However, the research progress of flapping-wing aircraft has lagged behind fixed-wing and rotor-wing aircraft due to the limitations of machine processing technology and the lack of theoretical research. Nowadays, with the development of materials technology, energy technology and related theories, more and more achievements have been made in the field of FAV. The emergence and development of FAV like Delfly[1], Roboraven[2], Robotic Hummingbird[3], Smartbird[4], etc. signifies that people have a deeper grasp of flapping-wing flight. Flapping-wing flight has become a research hotspot.

Compared with the fixed-wing flight and the rotor-wing flight, the flapping-wing flight mode has a better flight performance in low-speed flight field, including concealment, maneuverability, flight efficiency and wind resistance. FAVs in different sizes usually have different characteristics. Small-size FAV generally imitates insects and hummingbirds which has the characteristics of fast fluttering frequency and strong maneuverability. But it often has a small-size load capacity and cannot fly continuously for a long time. The large-size FAV which mimics birds like hawk, seagull, albatross, etc. has the characteristics of low flapping frequency, good load capacity and long flight endurance, and is more suitable for outdoor missions. Based on this goal, we designed the HITHawk, which inspired from the hawk in nature.

After 5-year's research, HITHawk has been able to achieve a continuous flight up to almost one hour, but its flight stability is not ideal. In order to further optimize the performance of the prototype, we developed an aerodynamic loads calculation method based on a state-space airloads theory developed by Peter et al.[5] which is used to calculate the aerodynamic loads under different working conditions. The state-space air loads theory is extended from classical thin airfoil theory, which is developed by Wagner[6], Theodorsen[7], Garrick[8], Isaacs[9], Greenberg[10] and Loewy[11] et al. This theory can be expressed in a matrix form which is similar to the dynamic equation, and it is easy to couple with structural dynamic equation.

Using this calculation method can help us finish the dynamic simulation and control law design. In order to verify the accuracy of this calculation method, the experiments which use the six-dimensional force sensor to measure the aerodynamic loads generated by HITHawk' s flapping wings under different working conditions is designed.

The remainder of the paper is organized as follows. Section II introduces HITHawk's structural parameters and flapping equation. Section III introduces the Peter's state-space airloads theory and shows the HITHawk's aerodynamic model design. Section IV exhibits and discusses the result of calculation and experiment. And the conclusion is given in Section V.

II. STRUCTURAL PARAMETER AND FLAPPING EQUATION

A. Structural Parameters

HITHawk is a large-size bionic flapping-wing robot independently developed by Harbin Institute of Technology(SZ)[12], as shown in Fig. 1. The flapping mechanism has only one degree of freedom(DOF). Both the lift and thrust required for flight are generated by the flapping wing. The tail is designed like a triangle and has two DOFs. Two control actuators are used to adjust the attitude of HITHawk. The structural parameters of the HITHawk are shown in Table 1.

*This work is supported by the National Natural Science Foundation of China (Grant No. U1613227), and Guangdong Special Support Program (Grant No. 2017TX04X0071) and Individual Maker Project of Shenzhen Maker Special Fund (AK24405057).

978-1-7281-6321-5/19//$31.00 ©2019 IEEE

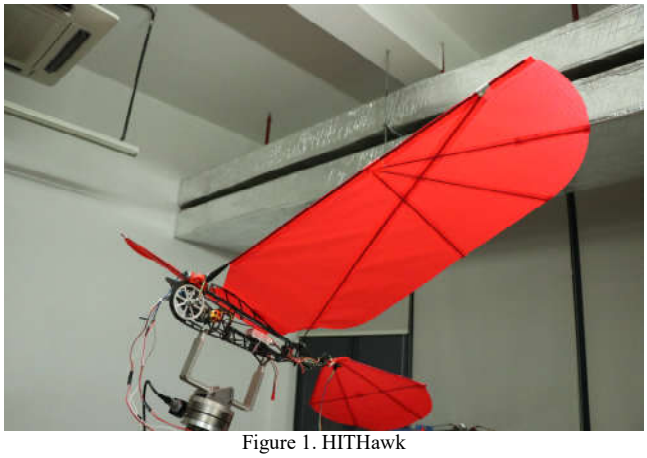

Figure 1. HITHawk

Table 1. Structural parameters of HITHawk

Parameters	Value
Total mass(g)	487
Wingspan(m)	1.6
Mean chord length(m)	0.3
Flapping frequency(Hz)	1-5
Load(g)	150
Flight endurance(min)	50

B. *Flapping Equation*

The 3-D view of driving mechanism model is shown in Fig. 2. In order to obtain the HITHawk's flapping kinematics, we use a micro-angle sensor with a sampling frequency of 500 Hz to detect the change of the flapping angle during one flapping cycle. The result is shown in Fig. 3.

According to Fig. 3, we can find that the change of the flapping angle is similar to the cosine curve. With the flapping frequency increases from 1Hz to 5Hz, the time proportion of the downstroke increased from 0.4 to 0.55. This is because when flapping frequency is low, the driving mechanism doesn't have enough energy to move smoothly. A resistance can be observed obviously during the upstroke. As the motor speed increases, the transmission becomes more lubricated, and the motor will rotate at a uniform speed. At this time, the flapping equation can be approximated to a cosine function:

$$\beta = 0.2392+0.3623\cos\left(2\pi t / T\right) \tag{1}$$

where β is the flapping angle. This cosine function will be used in the Section III as the flapping equation. The velocity and the acceleration of flapping angle is:

$$\dot{\beta} = -0.7246\pi\sin\left(2\pi t / T\right) / T \tag{2}$$

$$\ddot{\beta} = -1.4492\pi^2\cos\left(2\pi t / T\right) / T^2 \tag{3}$$

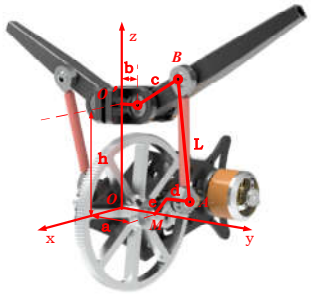

Figure 2. The 3-D view of driving mechanism model

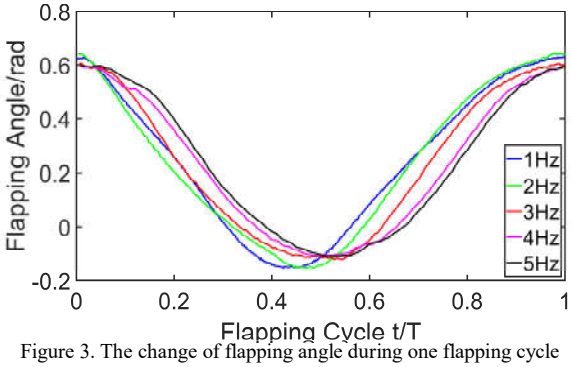

Figure 3. The change of flapping angle during one flapping cycle

III. AERODYNAMIC MODEL DESIGN

A. *Introduction of Peter's Air Loads Theory*

Nowadays, people always use computational fluid dynamics(CFD) to analyse the flow field[13]. CFD is a method for analysing, calculating and predicting flow field through computer numerical calculation. CFD can obtain the detail and the change of flow fluid flow clearly. However, CFD needs a large amount of computing resource and speeds long time to finish the calculation, which couldn't calculate the aerodynamic loads of FAV quickly. However, a state-space airloads theory developed by Peter et al. can compute far faster than CFD and does not need much computing resources. This method has a relatively high precision for calculating motions with large rigid motion and small flexible deformation such as flapping-wing flight, which is very suitable for HITHawk's dynamic simulation and control law design.

According to this method, the airfoil coordinate system is established, as shown in Fig. 4. The airfoil chord line is parallel to the x-axis and the mid-chord locates on the coordinate system origin. The wind velocity component along the positive x-axis direction is defined as u_0. The wind velocity component along the positive y-axis direction is defined as v_0. The velocity gradient caused by the rotation of the coordinate system is v_1, and the counterclockwise is positive. Then the vertical velocity can be expressed as $v_0 + v_1 x / b$, where b is the semi-chord. The deformations of

the airfoil $h(x,t)$ is positive along the negative direction of y-axis.

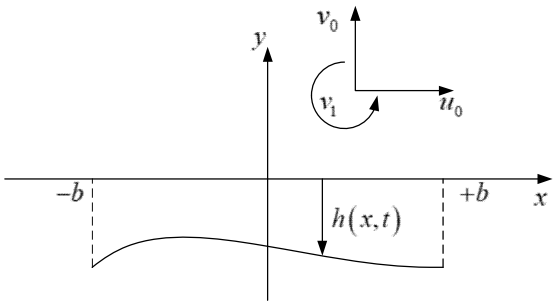

Figure 4. The airfoil coordinate system[14]

The nonpenetration boundary condition can be written directly as[5]

$$w = \overline{v} + \lambda = u_0 \partial h / \partial x + \partial h / \partial t + v_0 + v_1 x / b \tag{4}$$

where w is the total induced flow, $\overline{v}$ is a part of induced flow caused by trailed circulation. λ is the other part of induced flow caused by bound circulation.

Let $\varphi = \arccos(x/b)$, then using the Glauert change, we can get[15]

$$h = h_n \cos(n\varphi) \tag{5}$$

where n is the order of Glauert expansion. According to the Gauss-Chebyshev Integral Formula, h_n can be expressed as:

$$h_n = \left[k/(g+1)\right] \cdot \int_0^{\pi} h(\varphi)\cos(n\varphi)d\varphi \tag{6}$$

$$k = \begin{cases} 1 & n = 0 \\ 2 & n > 1 \end{cases} \tag{7}$$

where g is the number of gauss points on each airfoil (the position of Guass points will be discussed below). h_φ is the position function of each Guass point. It can be expressed in matrix form

$$\boldsymbol{h_n} = \boldsymbol{T_g} \bullet \boldsymbol{h_\varphi} \tag{8}$$

where T_g is a $(n+1)\times g$ integral matrix

$$\boldsymbol{T_g} = \begin{bmatrix} 1 & 1 & 1 & \cdots \\ \cos\varphi_1 & \cos\varphi_2 & \cos\varphi_3 & \cdots \\ \cos 2\varphi_1 & \cos 2\varphi_2 & \cos 2\varphi_3 & \cdots \\ \vdots & \vdots & \vdots & \ddots \end{bmatrix} \tag{9}$$

Using the Glauert change of variable, the pressure distribution can be expressed as:

$$\Delta P = 2\rho\left[\tau_0 (1-\cos\varphi)/\sin\varphi + \sum_{n=1}^{\infty} \tau_n \sin(n\varphi)\right] \tag{10}$$

where ρ is the air density, τ_n can be expressed by u_0, v_0, v_1, h_n and $\dot{h}_n$ [5].

Eventually, the aerodynamic force along the y-axis can be expressed as

$$F_y = \int_{-b}^{b} \Delta P dx = \int_0^{\pi} b\Delta P \sin(\varphi) d\varphi = 2\pi\rho b(\tau_0 + 1/2\tau_1)$$
$$= 2\pi\rho b\left(u_0 w_0 - u_0\lambda_0 + u_0 w_1/2 + b\dot{w}_0/2 - b\dot{w}_2/4\right) \tag{11}$$

The aerodynamic force along the y-axis is

$$F_x = \int_{-b}^{+b} (\Delta P)(\partial h/\partial x)dx - 2\pi\rho b(w_0 - \lambda_0)^2$$
$$= -2\pi\rho b\left(v_0 + \dot{h}_0 - \lambda_0\right)\left(v_0 + \dot{h}_0 - \lambda_0 + u_0 \sum_{n=1}^{\infty} n h_n / b\right)$$
$$+2\pi\rho \sum_{n=1}^{\infty} h_n \left[b\left(\ddot{h}_{n-1} - \ddot{h}_{n+1}\right)/4 + n u_0 \dot{h}_n + n\dot{u}_0 h_n/2\right]$$
$$+2\pi\rho h_1\left(b\dot{v}_0/2 + b\ddot{h}_0/4\right) + \pi\rho\left(b h_2 \dot{v}_1/2 + u_0 v_1 h_1\right) \tag{12}$$

B. HITHawk Aerodynamic Model

The deformation along the span is small when HITHawk's flapping frequency is lower than 5 Hz. In that situation the movement of flapping-wing can be simplified to the combination of plunge motion and the rotate motion around the leading edge. Along the span direction we divide the flapping wing uniformly into several parts and analyse the aerodynamic airloads of the airfoil in the section. As shown in Fig. 5. Assume that each part of the wingspan suffers the same aerodynamic loads along the wingspan direction, the sum of the aerodynamic loads of each part can be considered as the total aerodynamic loads.

For each two-dimensional airfoil in section, the position function $h(x,t)$ can be solved by the Gauss-Chebyshev integral formula. The motion of each Gaussian point is the combination of the plunge motion perpendicular to the x-axis and the rotate motion around the leading edge, as shown in Fig. 6. Define the function $F(x)$ to represent the shape of airfoil, which coincide with the camber line. The position function of each Gaussian point can be expressed as

$$h_\varphi = (b+x)\theta - z - F(x) \tag{13}$$

where θ is the rotate angle around the leading edge. z is the plunge motion of flapping wing, $z = y\beta$.

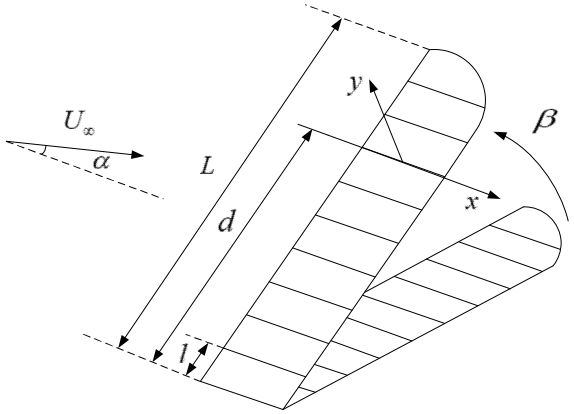

Figure 5. The flapping-wing coordinate system[9]

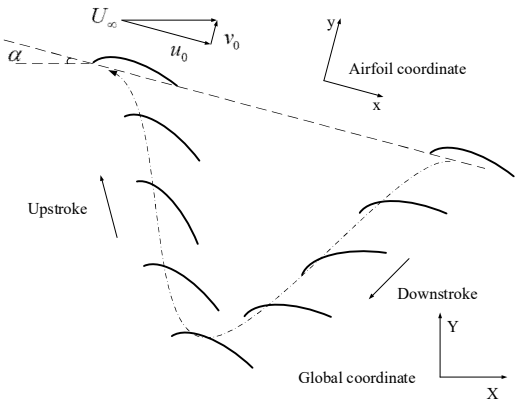

Figure 6. The motion of airfoil

The rotate angle θ is assumed to have a 90° phase difference compare to flapping angle β. When $\beta = 0$ in downstroke, θ reaches the minimum value. And θ is assumed to increase linearly along the direction of wingspan. Thus the expression of rotate angle θ can be written as:

$$\theta = -\theta_m d \sin(wt) / L \tag{14}$$

where θ_m is the maximum value of rotate angle at the wing tip. Which is set as 20°. d is the distance from the airfoil to the wing root.

The angle between the X-axis and the steady inflow U_∞ is the angle of attack α. According to the Fig. 6, we can get $u_0 = U_\infty \cos\alpha$, $v_0 = U_\infty \sin\alpha$. Regardless of the pitching motion of the HITHawk, the velocity gradient $v_1 = 0$.

For each two-dimensional airfoil, the calculated results of aerodynamic loads are relative to its airfoil coordinate system. In order to obtain the total aerodynamic loads received by both the left flapping-wing and the right flapping-wing, the aerodynamic loads obtained from each part need to be converted to the global coordinate system XOY, which the origin is set at the center of gravity of HITHawk (the position of the center of gravity of HITHawk can be obtained by the six-dimensional force sensor). The aerodynamic loads along the negative direction of X-axis is the thrust. And the aerodynamic force along the positive direction of Y-axis is the lift. Considering the symmetric flapping of the left and the right flapping-wing relative to the body, finally we can get

$$F_{lift} = \int_N (2F_y l \cos\alpha \cos\beta - 2F_x l \sin\alpha) \tag{15}$$

$$F_{thrust} = \int_N (-2F_x l \cos\alpha - 2F_y l \sin\alpha \cos\beta) \tag{16}$$

IV. CALCULATIONS AND EXPERIMENTS

A. Experimental Design

In order to ensure the stability of the flapping, we use DC power to provide the energy for HITHawk. The testing mechanism is shown in Fig. 7. The six-dimensional force sensor can detect the three-axis forces and moments. The sampling rate is 100 Hz.

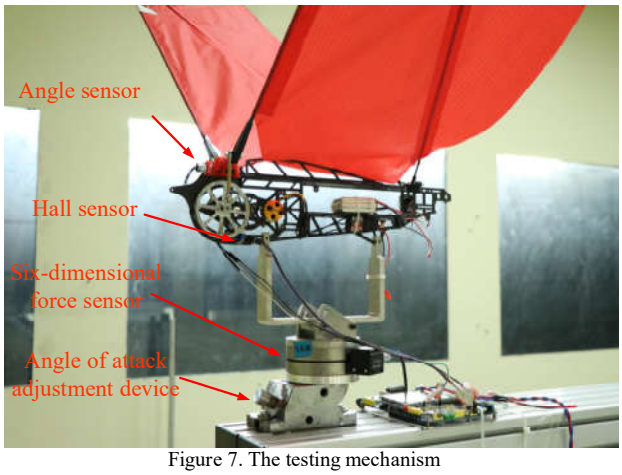

Figure 7. The testing mechanism

The measured data of the sensor is the sum of aerodynamic forces and inertial force of the flapping-wing. In order to eliminate the influence of inertial force, we designed a couple of flapping wings without fabric. The flapping wings has the same mass and center of gravity compare with the complete flapping wings. The value of experimental aerodynamic loads is the difference between the force data of complete flapping wings and the data of flapping wings without fabric at the same flapping frequency.

In order to eliminate the influence of vibration and reduce the interference effect of the wind tunnel wall, we make a $1.8m \times 0.5m \times 1.5m$ bulky pedestal. The test mechanism is fixed at a forward cantilever beam. Which can effectively reduce the interference of the pedestal to the flow field around the HITHawk. The wind tunnel experiments were carried out in the wind tunnel of Harbin Institute of Technology (Shenzhen). The test section of this tunnel is $24.0m \times 6.0m \times 3.6m$, the velocity field inhomogeneity and the turbulence are less than 1%, and the wind velocity can be controlled at 1-10m/s. Which is very suitable for wind tunnel testing of HITHawk's full-scale prototype. Fig. 8 shows the HITHawk in the wind tunnel.

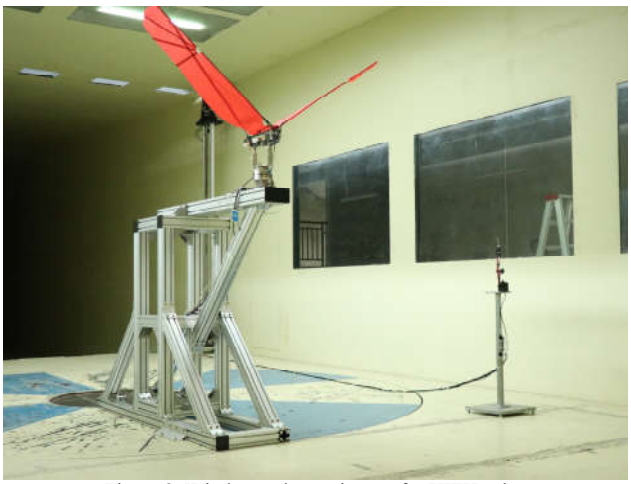

Figure 8. Wind tunnel experiments for HITHawk

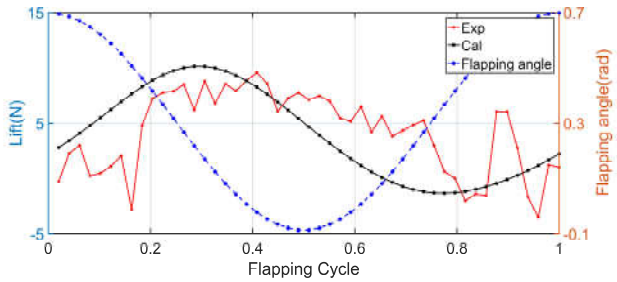

Figure 9. The lift in one flapping cycle

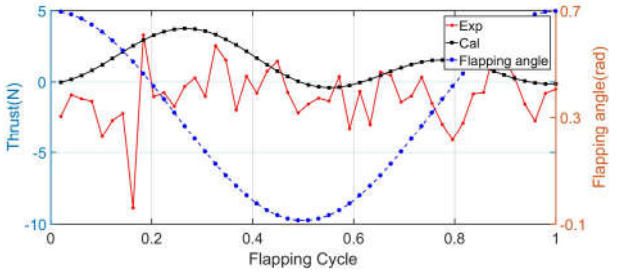

Figure 10. The thrust in one flapping cycle

Table 2. Mean lift and mean thrust

	Mean lift(N)	**Mean thrust(N)**
Calculation	4.581	0.934
Experiment	4.195	-1.028

B. Aerodynamic Loads in One flapping Cycle

Both the calculation and experiment get the results when the wind velocity is 5 m/s, the angle of attack is 10° and the flapping frequency is 2 Hz. The lift and thrust in one flapping cycle is shown in Fig. 9 and Fig. 10. And the mean lift and mean thrust is shown in Table 2. The flapping wings used in this situation is named as flapping wing A. As shown in Fig. 8. The lift produced by flapping wing A is approximately equal to the gravity of HITHawk. There exists a phase difference between experimental curve and calculation curve.

It can be seen from Fig. 9 that the lift of the calculated value and the experimental value are relatively close, and the peak of the lift occurs when the flapping wing A reaches the fastest speed in downstroke. The change of lift is relatively gentle when in upstroke. It can be seen that the flapping in upstroke is slower than flapping in downstroke when there comes the incoming flow. Both the lift and thrust changing slowly in upstroke.

C. Aerodynamic Loads in Different Working Conditions

Fig. 11 shows the mean lift and mean thrust in different working conditions. In Fig. 11.a to b, the wind velocity is kept in 5 m/s and the flapping frequency is kept in 2 Hz. As the angle of attack increases in range of 0° to 20°, the mean lift increases and the mean thrust decreases, which accord with the actual flight performance.

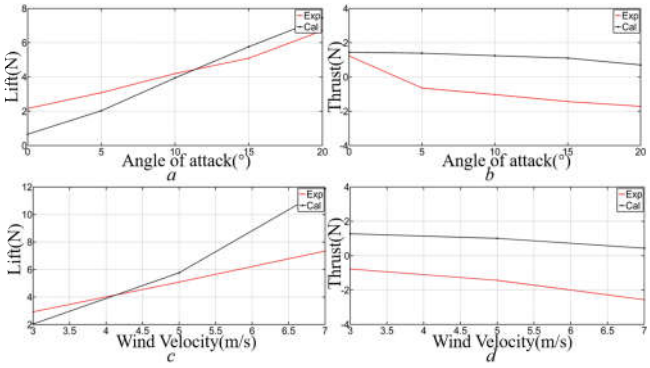

Figure 11. Mean lift and mean thrust in different situation

However, for thrust calculation, there exists an error near 2N, which need us to correct model to reduce the error in the further research work.

Fig. 11.c to d show that as the wind velocity increases in range of 3 m/s to 7m/s, the mean lift increases and the mean thrust decreases. The angle of attack is kept in 15° and the flapping frequency is kept in 2 Hz. When the wind velocity is greater than 5 m/s, there is a large error between the calculated mean lift and the experimented mean lift. That is because the current calculation method simplifies the complex flexible deformation of flapping wings into a simple pitching motion. When the wind velocity is small, the flexible deformation is small enough so that using this simplification has a good precision to calculate aerodynamic loads. However, when the wind velocity becomes fast, the deformation along the wingspan is not negligible, and this simplification is not suitable. As shown in Fig. 11.d, there also exists an error near 2N between the calculation results and experimental results. Inaccurate calculation models and large experimental vibrations lead to this error primarily.

D. Aerodynamic Loads for Different Flapping Wings

Reference to birds in nature, we designed a series of flapping wing ribs, which made by carbon fiber, as shown in Fig. 12. The airfoil with large camber is used in the inner position of flapping wing while the airfoil with small camber is used in outer position.

The upper surface of the ribs is sticked to the fabric of flapping wing by adhesive. While in lower surface there are two methods, as shown in Fig. 13. The first method is sticking nothing. In this situation we consider the upper of the ribs as the airfoil to calculate the aerodynamic load. And the flapping wing is named flapping wing B. The second method is sticking the lower surface of the ribs with another fabric so that the flapping wings can form complete and thick airfoil. The flapping wing is named flapping wing C. And in calculation we use the camber line to replace the airfoil. The result of calculation and experiment is exhibited in Fig. 14. The wind velocity is 5 m/s, the angle of attack is 10° and the flapping frequency is 2 Hz.

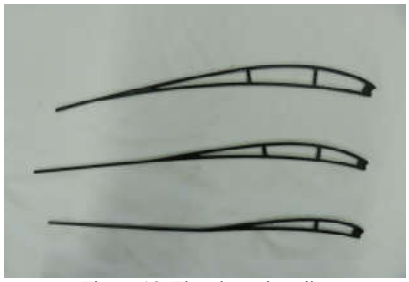

Figure 12. Flapping wing ribs

a *b*

Figure 13. Flapping wing B and flapping wing C

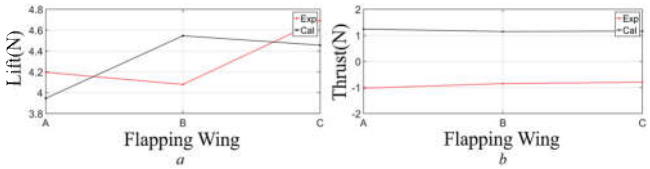

a *b*

Figure 14. Mean lift and thrust generated by flapping A, B and C

From Fig. 14 we can see that the flapping wing C is able to generate more lift, while the thrust generated by flapping wing A is slightly larger than B and C. Actual flight test indicates that flapping wing C has the best aerodynamic efficiency but its wind resistance is not good, which verifies the results of the experiments and calculations.

The calculation results of the lift of the flapping wings A and C are in good agreement with the experimental values, but the calculation results of the flapping wing B are not sufficiently accurate. That illustrates that using the upper of the ribs as the airfoil to calculate the aerodynamic load is incorrect for this kind of flapping wings which the airfoil is not complete.

V. CONCLUSION

In this paper, a method for aerodynamic loads calculation of flapping wing based on a state-space air loads theory was exhibited. This method provided a relatively high precision for calculating motions with large rigid motion and small flexible deformation and was suitable for HITHawk's aerodynamic loads calculation. Based on this method, we calculated the aerodynamic loads for HITHawk in different working conditions and designed a series of verification experiments. Compared the calculated results with experimental results, we found that this calculation method has a good approximation of lift when the wind velocity was less than 5 m/s. While the calculation of thrust needs to be more accurate.

There still exists insufficiency in this paper. The vibration of HITHawk body in experiments has great influence on the accuracy of experimental results. The effect of the flapping inertial force is not well eliminated. And the flexible deformation of the flapping wing is not well approximated when the wind velocity is greater than 5 m/s. In the future, we will perfect experimental design to provide more realistic data and introduce structural simulation to improve the calculation accuracy.

REFERENCES

[1] M. Karásek, F. T. Muijres, C. De Wagter, B. D. W. Remes, and G. C. H. E. de Croon, "A tailless aerial robotic flapper reveals that flies use torque coupling in rapid banked turns," vol. 361, no. 6407, pp. 1089-1094, 2018.

[2] J. Gerdes, A. Holness, A. Perez-Rosado, L. Roberts, and S. K. J. S. R. Gupta, "Robo Raven: A Flapping-Wing Air Vehicle with Highly Compliant and Independently Controlled Wings," vol. 1, no. 4, pp. 275-288, 2014.

[3] Z. Jian, F. Fan, T. Zhan, and X. Deng, "Design optimization and system integration of robotic hummingbird," in IEEE International Conference on Robotics & Automation, 2017.

[4] Smartbird homepage, https://www.festo.com/group/en/cms/10238.htm.

[5] Peters D A, Hsieh M, and Torrero A. A State-Space Airloads Theory for Flexible Airfoils[J]. Journal of the American Helicopter Society, 2007, 52(4): 329–342.

[6] H. Wagner, "Über die Entstehung des dynamischen Auftriebes von Tragflügeln," vol. 5, no. 1, pp. 17-35, 1925.

[7] T. Theodorsen, "General Theory of Aerodynamic Instability and the Mechanism of Flutter," NACA Report 496, pp. 413-433, 1949.

[8] I. E. J. T. R. A. Garrick and I. Library, "Propulsion of a Flapping and Oscillating Airfoil," 1936.

[9] R. J. J. o. t. A. S. Issacs, "Airfoil theory for rotary wing aircraft," vol. 13, no. 4, pp. 218-220, 1946.

[10] J. M. J. T. R. A. Greenberg and I. Library, "Airfoil in sinusoidal motion in a pulsating stream," 1947.

[11] R. G. J. J. o. t. A. S. Loewy, "A two-dimensional approximation to the unsteady aerodynamics of rotary wings," vol. 24, no. 24, 1957.

[12] E. Pan, L. Chen, Z. Bing, and W. Xu, "A Kind of Large-Sized Flapping Wing Robotic Bird: Design and Experiments," 2017.

[13] W. Yuan, M. J. C. A. Khalid, and S. Journal, "Preliminary computational fluid dynamics (CFD) studies of flapping-wing aerodynamics," vol. 54, no. 3/4, pp. 51-63, 2008. [M]. Cambridge: Cambridge University Press, 2008.

[14] Stanford B, Beran P, Kobayashi M. Aeroelastic Optimization of Flapping Wing Venation:A Cellular Division Approach [J]. AIAA Journal, 2015, 50(4):938-951.

[15] Katz J, and Plotkin A. Low-Speed Aerodynamics [M]. Cambridge, England: Cambridge Univ.Press, 2001.